



IMAGE FUSION BASED ON JOINT NONSUBSAMPLED CONTOURLET AND OVERCOMPLETE BRUSHLET TRANSFORMS

Zhang Pai

School of Intelligence and Information Engineering

Tangshan University, Private bag 17

Tangshan, China

Emails: raindrop_pai@qq.com

Submitted: July 12, 2015

Accepted: Jan. 11, 2016

Published: Dec. 1, 2016

Abstract- This paper proposed an image fusion method based on a novel scheme with joint nonsubsampling contourlet and overcomplete brushlet transform. And an improved region energy operator is employed as the fusion strategy, which can take full advantage of the anisotropic texture information and multidimensional singular information in the new multiresolution domain. Experimental results show that the proposed method improved the fusion results not only in visual effects but also in objective evaluating parameters.

Index terms: Non-subsampled contourlet transform, Over-complete brushlet transform, image fusion, region energy feature.

I. INTRODUCTION

Image fusion is the process by which two or more images are combined into a single image retaining the important features from each of the original images. The fusion of images is often required for images acquired from different instrument modalities or capture techniques of the same scene or objects. Important applications of the fusion of images include medical imaging, microscopic imaging, remote sensing, computer vision, and robotics.

Most of fusion techniques are based on combining the multiscale decompositions (MSD) of the source images. MSD-based fusion schemes provide much better performance than the simple methods studied previously. Recently many new MSD transforms are introduced in image fusion (i.e., bandelet, curvelet, contourlet, etc.) [1] to overcome the limits of original discrete wavelet transform. Contourlet was recently pioneered by Do [2]. Compared with wavelet, it provides different and flexible number of directions at each scale and can capture the intrinsic geometrical structure. However, the original contourlet lacks shift-invariance and causes pseudo-Gibbs phenomenon around singularities. Nonsub-sampled contourlet transform (NSCT) [3], as a fully shift-invariant form of contourlet, leads to better frequency selectivity and regularity. Brushlet [4] is new biorthogonal bases which are obtained by segmenting the Fourier plane [5-7]. It can achieve precise representation of the image in terms of oriented textures with all possible directions, frequencies, and locations, but the original brushlet transform also lacks shift-invariance [8-9] and yields blocks artificial phenomenon. Here we adopt the overcomplete brushlet transform (OCBT) [10] as a remedy for the problem.

In this paper, we first project a novel scheme with joint NSCT and OCBT. The motivation of the proposed MSD transform not only can represent the geometrical features such as edges and textures more sparsely but also capture and preserve the anisotropic edges information and detail directions of images effectively. The proposed scheme decomposition coefficients can also highlight the energy features more effectively than other traditional MSD coefficients. In terms of these excellent properties, we apply it in fusing multifocus and medical images, and employ an improved region energy features as the fused strategy. The fusion process is divided into several stages. In the first stage, the source images are decomposed by NSCT, then we obtain the coefficient matrix of all directional subbands at each of high frequency levels. Here, each of coefficient matrix represents its directional information. Considering the source images may

include lots of details, the coefficient matrices in the NSCT domain also embody complex directions and textures information[11-12]. In order to highlight salient features of each directional subband, OCBT is employed to decompose all the directional subbands at each high frequency level in NSCT domain. Then the obtained coefficient matrices here can fully represent the feature information of all possible directions, frequencies, and locations. In the second stage, we select all the coefficient matrices and divide them into subregions with a uniform suitable size. Then the subregions which are located in the same location of the same directional subbands across all high frequency levels are picked out to calculate and aggregate their region energy values. In the last stage, a hybrid region and pixel energy values used as the match measure parameters are employed to obtain high-frequency and low-frequency fused coefficients respectively. Finally, the fused image is reconstructed by inverse OCBT and NSCT successively. Experimental results show that the proposed algorithm outperforms the existing energy-based image fusion algorithms. (i.e., global energy merging-based fusion algorithm (GEB)[13], a region-based multisolution image fusion algorithm (REMR)[14] and sum-modified-laplacian-based multifocus image fusion algorithm in cycle spinning sharp frequency localized contourlet transform domain (SML_SFLCT)[15]). and also is visually superior to other mentioned methods.

II. PRINCIPLE OF NSCT AND OCBT

In the foremost contourlet transform, downsamplers and upsamplers are presented in both the laplacian pyramid (LP)[16] and the directional filter banks (DFB)[17]. Thus, it is not shift-invariant, which causes pseudo-Gibbs phenomenon around singularities. NSCT is an improved form of contourlet transform.

In contrast with contourlet transform, nonsubsampling laplacian pyramid (NLP)[18-21] structure and nonsubsampling directional filter banks (NDFB)[22-23] are employed in NSCT. The NLP structure is achieved by using two-channel nonsubsampling 2D filter banks. The NDFB is achieved by switching off the downsamplers/upsamplers in each two-channel filter bank in the DFB tree structure and upsampling the filters accordingly. As a result, NSCT is shift-invariant and leads to better frequency selectivity and regularity than contourlet transform. figure.1 shows the decomposition framework of NSCT.

Brushlet functions, first introduced by Coifman and Meyer for compression of highly textured images, are well localized in both time and frequency. The major difference between the brushlet basis and wavelet packets is the arbitrary tiling of the time-frequency plane and the perfect localization of a single frequency in one coefficient. Brushlets is a complex valued function with a phase. The phase of the 2D brushlet provides valuable information about the orientation. These properties make the brushlets suitable for texture and directional image analysis.

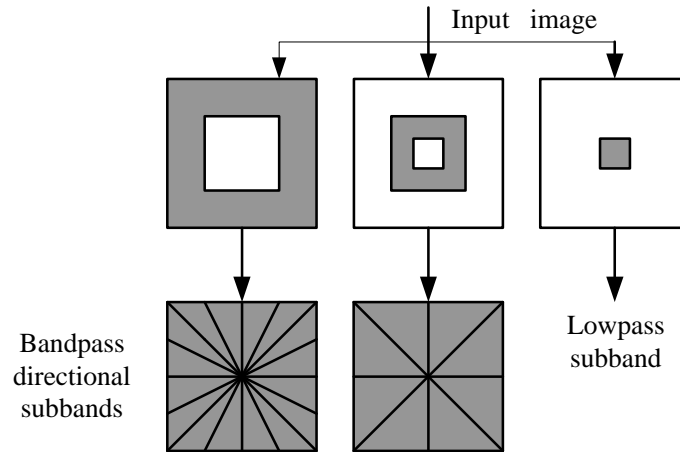


Figure 1. Decomposition framework of NSCT

Here, In order to illustrate the orientation selective property of the 2D brushlet, we have calculated the brushlet expansion of an image named Lena (see figure. 2).

A first expansion was performed with a partitioning of the Fourier plane into four quadrants. The

four sets of brushlets have the orientation $\frac{\pi}{4} + k \frac{\pi}{2}$, $k = 0, 1, 2, 3$. A second expansion has been

performed by using a finer grid. Each quadrant was further divided into four sub-quadrants. The

sixteen set of brushlets have twelve different orientations. The orientations $\frac{\pi}{4} + k \frac{\pi}{2}$ are associated

with two different frequencies. The four lattice squares around the origin characterize the DC terms of the expansion. The other squares correspond to higher frequency.

Brushlets has been proven efficient in texture and directional image analysis. In the process of brushlet transform, it need to select the overlapping subintervals of the Fourier plane and expand them into a local Fourier basis. This can cause the aliasing effects. To avoid this and at the same time increase the number of coefficients for the same subinterval size along each dimension, Elsa D. Angelini etc. projected onto an extended Fourier basis adopted it to construct a new scheme of

brushlet transform called overcomplete brushlet transform(OCBT).The basic idea of this new transform is stated as follows:

The overcomplete projection is efficiently implemented by padding the folded signals with zeros along each dimension and computing its Fourier transform(FT)[24-25]. Since padding a signal will increase the resolution of the FT, overcomplete projections increase the number of coefficients for the same interval and therefore, increase resolution in the transform (coefficient) plane. For an overcomplete projection, each subinterval of the Fourier domain is projected onto a brushstroke of dimension equal to the original number of elements. The orientation and size of the original brushstroke are preserved, as the phase of the brushstroke is not modified. However, the number of points defining each brushstroke in 2D is increased to match the original size of the volumetric data. Inside a subvolume of the FT, the coefficients are stored in the same manner as the data points in the original signal.

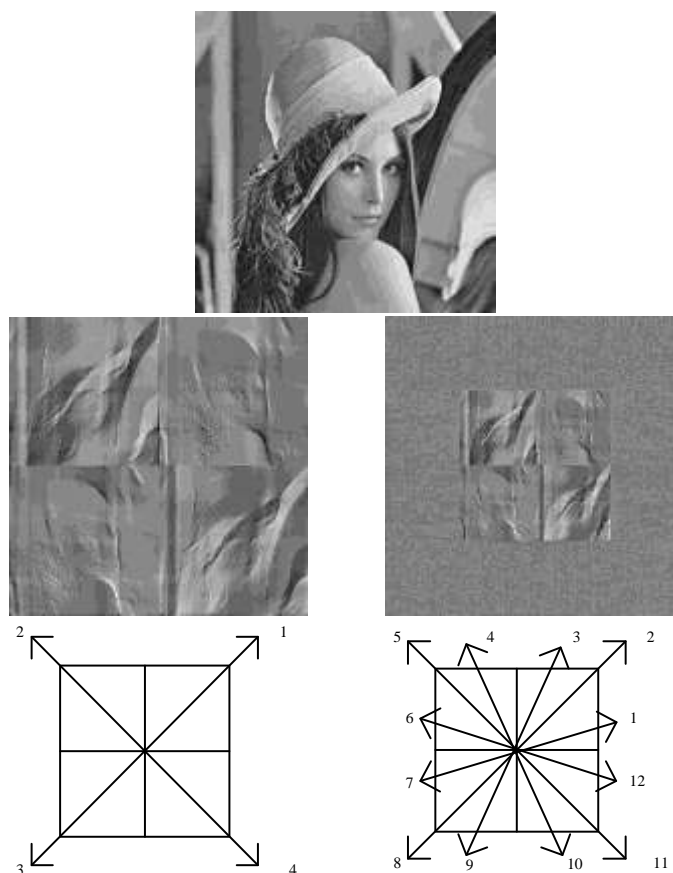


Figure 2. Brushlet decompositions(imaginal parts) of Lena and their associated directions. From top to bottom: Original image of Lena; Level 1 decomposition; Level 2 decomposition.

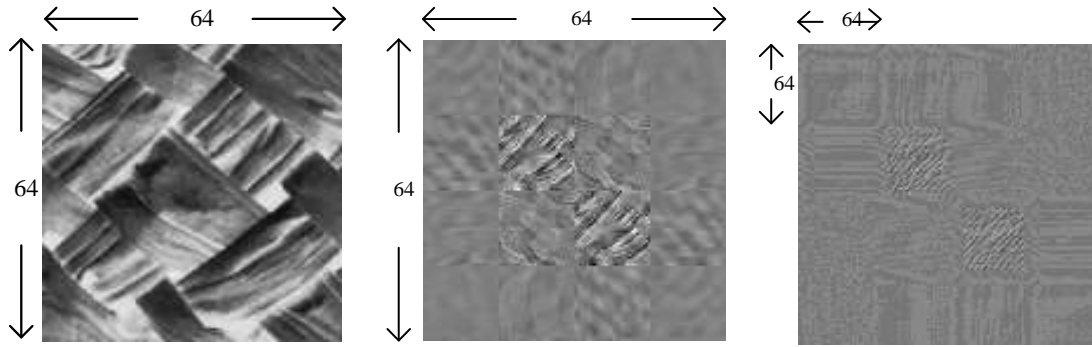


Figure 3. Decimated and overcomplete brushlet analysis with (4×4) tiling of the Fourier plane.

From left corner to right corner: Original image of size (64×64) , The 16 coefficient planes for a decimated brushlet analysis. Each coefficient quadrant is of dimension (16×16) , four times smaller than the original image. The 16 coefficient planes for an overcomplete brushlet analysis.

Each coefficient quadrant is of dimension (64×64) , the same size as the original image.

Therefore, in the overcomplete case, there is a perfect homomorphism between the location of data points in the original set and the position of the coefficients in each projected subvolume. OCBT as an overcomplete multiscale representation is suited for image analysis and yields a translation invariant representation, as observed in figure. 3.

III. IMAGE FUSION ALGORITHM BASED ON JOINT NSCT AND OCBT TRANSFORMS

Region-based and pixel-based energy algorithms in multiresolution decomposition (MSD) domain have proven to be very useful for image fusion. However, two problems existing in these methods have confused us. One of them is that, in the majority of applications, we are interested in the representation of the objects which are often possessed of complex details and no matter employ what kind of individual energy-based fusion methods could not accurately fuse them. The other problem is, in what kind of the MSD domain, these energy-based fusion methods are the most effective for image fusion.

Firstly, to overcome the first disadvantage, it is reasonable to come up with an idea of incorporating the pixel and region information into fusion process. We project a strategy with two

steps. For the step one, an energy value of each matrix region with suitable size is calculated in the MSD domain. Then, in terms of a certain rule, we pick out the regions which are located in the place of clear parts and blurry parts of source images and use a pixel energy-based fusion method to handle the coefficients. This new strategy can capture and preserve the anisotropic edge information and detail direction texture of collected images effectively.

Then, to settle the second problem, a novel scheme with joint NSCT and OCBT is proposed. First the source images are decomposed into different frequency subbands by the NLP, and then the high frequency subband is further decomposed into directional subbands by NDFB. Next, the OCBT is taken on each directional subband. The directional subbands in NSCT provide excellent directional details information of high frequency levels for source images. And overcomplete brushlet is a complex valued function with a phase. The phase of the 2D brushlet provides valuable information about the orientation. These properties make the brushlets suitable for texture and directional image analysis. Therefore, in the directional subbands at each high frequency level, the coefficient matrices which are achieved by combining these two multiresolution transforms can represent the geometrical features such as edges and texture more sparsely. In addition, NSCT and OCBT are both shift-invariant, when a local energy operator is provided as the fusion strategies to handle the coefficient matrices, it will not yield blocks artificial phenomenon and capture the region detail information accurately.

The proposed fusion algorithm can be divided into four different stages with reference to figure.4.

Stage I

- 1) Read the two source images A and B to be fused.
- 2) Make source images via NSCT and illustrate one of them, the mapping is assumed to be of the form:

$$x^0 \rightarrow \{y^1, y^2, \dots, y^K, x^K\} \quad (1)$$

where, y^k is the detail image at level k and x^K is the approximation at the coarsest level K. Then y^k , $k = 1, 2, \dots, K$ is further separated into subbands according to its orientation, namely, $y^k = \{y_1^k, y_2^k, \dots, y_D^k\}$ representing D directions. Here the number of directional subbands at all high-frequency levels is the same with each other, which is for preparation of combination of region-based energy values in the same directional subband across levels.

3) $y_d^k, d \in [1, D] k \in [1, K]$ are decomposed by a level 2 OCBT. Consider that the overcomplete brushlets are complex functions .so we obtain both real part and imaginary part brushlets coefficient matrices, namely: $yBreal_d^k, yBimg_d^k, d \in [1, D] k \in [1, K]$.

Stage II

1) Divides $yBreal_d^k$ into subregions which can be denoted as $\{yBreal_d^k(1), yBreal_d^k(2), \dots, yBreal_d^k(P)\}$, P is the num of subregions. then we caculate the energy values of $yBreal_d^k(p), p \in [1, P]$. $yBimg_d^k$ is made the same deal with $yBreal_d^k$ and obtain $yBimg_d^k(p)$. Assume that $yBreal_d^k(p)(i, j)$ and $yBimg_d^k(p)(i, j)$ represent each real part and imaginary part coefficient respectively in pth subregion. The energy value is calculated by using following formula:

$$E_d^k(p) = \sum_{i \in I, j \in J} \left(yBreal_d^k(p)(i, j)^2 + yBimg_d^k(p)(i, j)^2 \right) \quad (2)$$

where I, J are sizes of subregions.

2) Combine energy values of the subregions which are located in the same position of the same directional subbands at all high-frequency levels. the algorithm is calculated as follows:

$$Sum_E_d(p) = \sum_{k \in K} E_d^k(p) \quad (3)$$

Stage III

1) Assum $Sum_E_d^{(1)}(p)$ and $Sum_E_d^{(2)}(p)$ are from source image A and B respectively. By comparing these two energy values , a map matrix can be generated:

$$map(p) = \begin{cases} 1 & Sum_E_d^{(1)}(p) \geq Sum_E_d^{(2)}(p) \\ 0 & Sum_E_d^{(1)}(p) < Sum_E_d^{(2)}(p) \end{cases} \quad (4)$$

the map matrix size is decided by the number of subregions. and each element of matirx is a match measure parameter which represents which corresponding subregion of source images should be adopted in the fused image.

2) Considering that the detail complexity of source image ,which may yield some miscarriage of justice in some subregions if only use the region-based energy algorithm as the fuse approach, and therefore cause fuzzy details and contours appeared in the fused image. To slove these two problems, we project two effective rules to deal with the map matrix, which are stated as follows:

firstly , a 3×3 window filter of the form $W = \begin{bmatrix} 1 & 1 & 1 \\ 1 & 1 & 1 \\ 1 & 1 & 1 \end{bmatrix}$ is proposed and used to filter the map

matrix. for certain subregions, their corresponding elements values in the matrix are different from all the neighbors' around them. We regard this situation as a miscarriage of justice. the approach can solve the problem. Equation(5) is a statement of the concrete rule.

$$map(p) = \begin{cases} 1 & \text{if } \sum_{\substack{i \in [-1,1] \\ j \in [-1,1]}} map(p+i, p+j) \geq 6 \\ 0 & \text{else} \end{cases} \quad (5)$$

Then, taking into account the contours and textures often appear at the staggered place of clear regions and fuzzy regions in source images. We employ a rule to pick out corresponding elements of these subregions in map matrix.

$$map(p) = \begin{cases} 1 & \text{if } \sum_{\substack{i \in [-1,1] \\ j \in [-1,1]}} map(p+i, p+j) \geq 7 \\ 0 & \text{if } \sum_{\substack{i \in [-1,1] \\ j \in [-1,1]}} map(p+i, p+j) \leq 3 \\ 3 & \text{if } 3 < \sum_{\substack{i \in [-1,1] \\ j \in [-1,1]}} map(p+i, p+j) < 7 \end{cases} \quad (6)$$

when it encounters $map(p) = 3$, that means the corresponding subregion is located in staggered place of clear regions and fuzzy regions of source images. These subregions are often composed of both clear part and fuzzy part coefficients, therefore, it , as a whole subregion ,is hard to be classified. To better preserve the details of these subregions .We hence abandon the proposed region energy values measure maximum(REM)-based rule. and employ pixel energy values measure maximum(PEM)-based rule to calculate each of coefficients energy values of the subregions .And by comparing each coefficient energy value of subregions from two source images, it can distinguish the coefficients which are from the clear parts or blurry parts of images more accurately.

3) The approach of PEM is stated as follows:

$$E_pixel_d^k(p)(i, j) = \sum_{\substack{p \in [-1,1] \\ q \in [-1,1]}} \left[yBreal_d^k(p)(i+p, j+q)^2 + yBimg_d^k(p)(i+p, j+q)^2 \right] \quad (7)$$

(i, j) is the coefficient orientation of subregions.

4) Choose a appropriate measure maximum-based rule in term of the elements of map matrix.

The fusion rule is chosen by :

$$Fusion_rule = \begin{cases} REM & \text{if } map(p) = 0 \text{ or } 1 \\ PEM & \text{if } map(p) = 3 \end{cases} \quad (8)$$

Assum $(yBreal_d^{(1)k}(p), yBimg_d^{(1)k}(p))$ and $(yBreal_d^{(2)k}(p), yBimg_d^{(2)k}(p))$ are from source image A and B respectively and the REM is implemented as follows:

$$yBreal_d^k(p) = \begin{cases} yBreal_d^{(1)k}(p) & \text{if } map(p) = 1 \\ yBreal_d^{(2)k}(p) & \text{if } map(p) = 0 \end{cases} \quad (9)$$

$$yBimg_d^k(p) = \begin{cases} yBimg_d^{(1)k}(p) & \text{if } map(p) = 1 \\ yBimg_d^{(2)k}(p) & \text{if } map(p) = 0 \end{cases} \quad (10)$$

Assum $E_pixel_d^{(1)k}(p)(i, j)$ and $E_pixel_d^{(2)k}(p)(i, j)$ represent the coefficient energy values of source image subregions respectively. PEM is implemented as follows:

$$yBreal_d^k(p)(i, j) = \begin{cases} yBreal_d^{(1)k}(p)(i, j) & \text{if } E_pixel_d^{(1)k}(p)(i, j) \geq E_pixel_d^{(2)k}(p)(i, j) \\ yBreal_d^{(2)k}(p)(i, j) & \text{if } E_pixel_d^{(1)k}(p)(i, j) < E_pixel_d^{(2)k}(p)(i, j) \end{cases} \quad (11)$$

$$yBimg_d^k(p)(i, j) = \begin{cases} yBimg_d^{(1)k}(p)(i, j) & \text{if } E_pixel_d^{(1)k}(p)(i, j) \geq E_pixel_d^{(2)k}(p)(i, j) \\ yBimg_d^{(2)k}(p)(i, j) & \text{if } E_pixel_d^{(1)k}(p)(i, j) < E_pixel_d^{(2)k}(p)(i, j) \end{cases} \quad (12)$$

$yBreal_d^k(p)$ and $yBimg_d^k(p)$ represent the real part and the imaginary part coefficients of subregions in each directional subband at all high-frequency levels respectively.

Stage IV

1) Use the selected-out $yBreal_d^k$ and $yBimg_d^k$ via inverse OCBT to obtain the y_d^k which represents the coefficients matrix in d directional subband at k level in NSCT domain.

2) we adopt the fusion rule mentioned above to fuse the low pass subband in NSCT domain and obtain coefficient matrix $x(K)$. the fused process is similar with the one in high frequency levels.

Taking into account the limited space, not repeat them here.

3) Use the selected-out $x(K)$ and y_d^k to reconstruct the fused image via inverse NSCT .

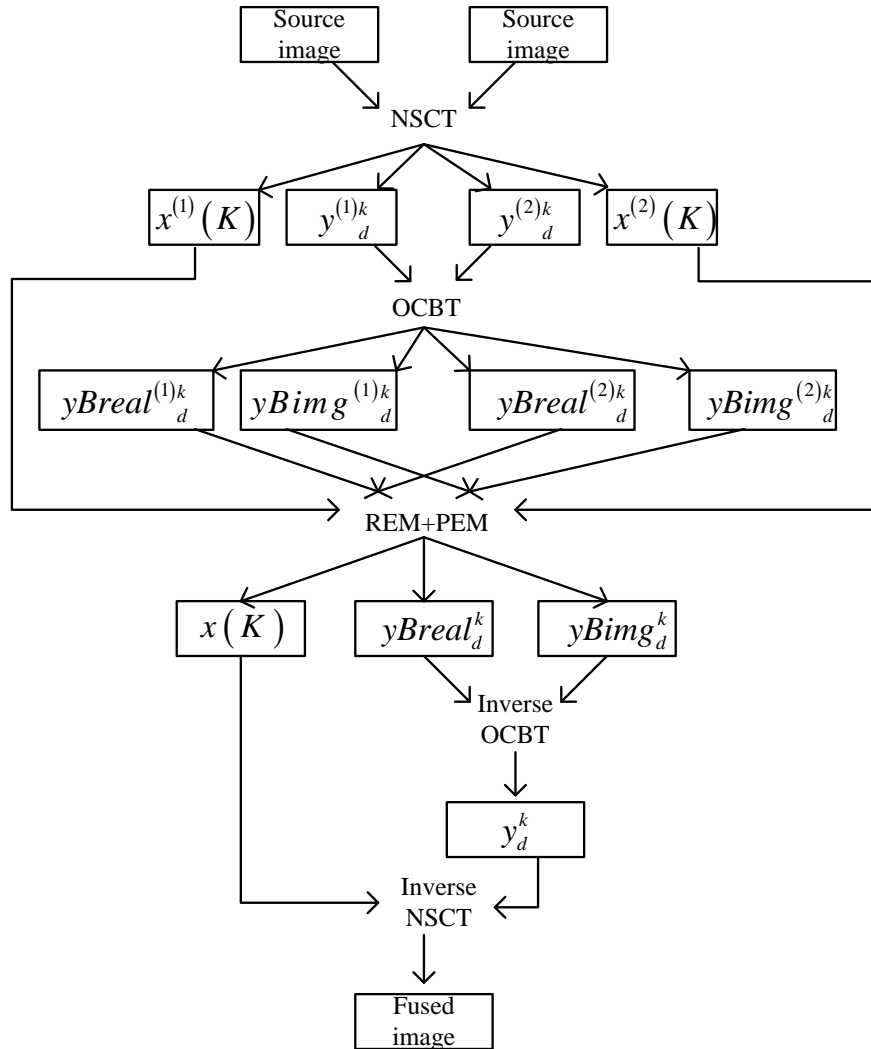


Figure 4. Schematic diagram of proposed fusion algorithm

IV. EXPERIMENTAL RESULTS AND ANALYSIS

The performance evaluation criteria of image fusion are still a hot topic in the research of image fusion, besides visual observation, mutual information(MI) [25], and $Q^{AB/F}$ [26] are used as information-based objective criteria. The reason is that image fusion aims at combining information and these criteria do not require the information of ideal fused image. MI essentially computes how much information from source images is transferred to the fused image,

whereas $Q^{AB/F}$ computes and measures the amount of edge information transferred from the source images to the fused images using a sobel edge detector.

To evaluate the performance of the proposed fusion algorithm, it is compared with GEB, REMR and SML_SFLCT image fusion algorithms. Objective criteria on MI and $Q^{AB/F}$ are listed in Table 1. Table 1 shows that MI and $Q^{AB/F}$ values of the proposed algorithm are the largest. It proves that the fused image of the proposed algorithm is strongly correlated with the source images and more image features are preserved in the fusion process. When all is said and done, our proposed algorithm outperforms other algorithms, no matter in visual observation and objective evaluation criterion.

TABLE 1. Comparison of objective criteria of different fused methods

Images	Fused method				
	Criteria	GEB	REMR	SML	Proposed
ClockA/B	MI	6.6301	7.0804	7.4092	8.3787
	$Q^{AB/F}$	0.6819	0.7183	0.7270	0.7439
LenaA/B	MI	5.5934	6.1809	6.3520	7.4982
	$Q^{AB/F}$	0.5640	0.6007	0.6371	0.7023
HoedA/B	MI	6.9538	7.0110	7.4139	7.5589
	$Q^{AB/F}$	0.6712	0.6859	0.7786	0.8008
CT&MIR	MI	3.0298	4.0209	4.2105	4.3625
	$Q^{AB/F}$	0.6146	0.6314	0.6783	0.7343

We select three multi-focus images (256×256 in size and 256 levels in gray) for testing. One of the fusion results using source image clocks are shown in figure.5 .From figure.5, It can be seen that fused image of GEM fusion method is not satisfactory in visual observation. The reason is that difference between multi-focus images is slight and transitional regions often exist because of many vague pixels. Coefficients are inaccurately selected using only region features as the fused strategy. And REMR methods is also not excellent in visual appearance for its MSD schemes is shift-variant. Though SML_SFLCT outperforms other two methods , NSCT lacks a better representation of the contours and textures than the joint NSCT and OCBT schemes, so its fused image is not clearer and more natural than the proposed fused results. Our experiments show that the proposed approach outperforms other fused method in visual effect.

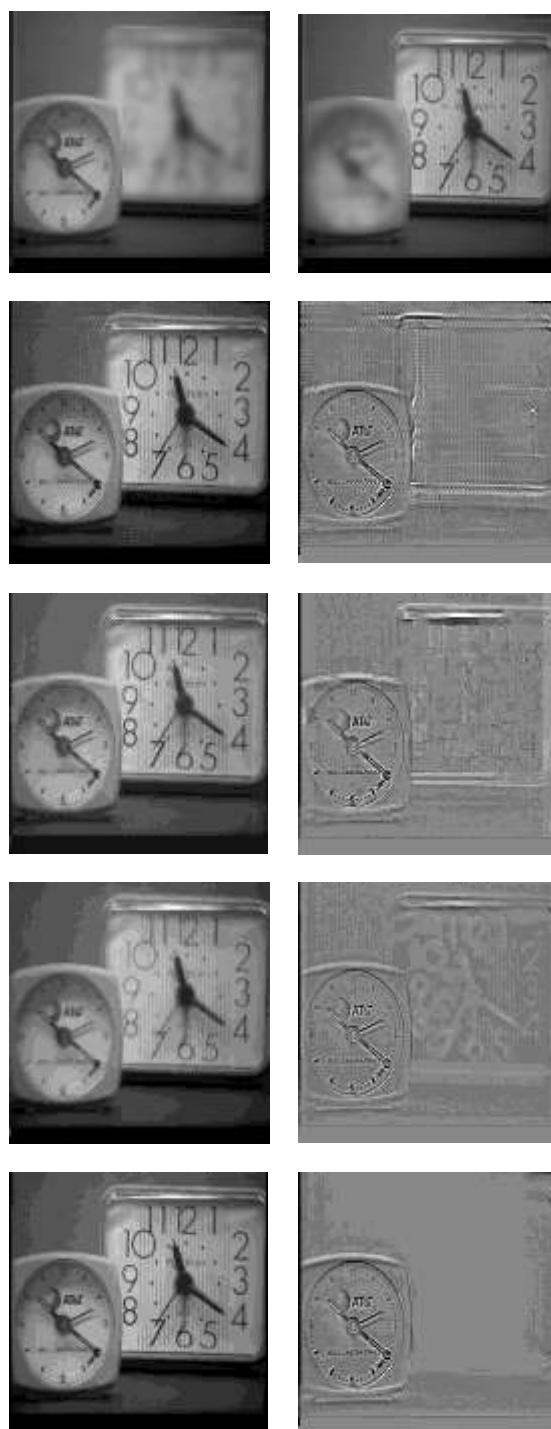


Figure 5. Multifocus image fusion results

From top left corner to bottom right corner: clockA.tif: focus on left; clockB.tif: focus on right;
 Fused images using GEB, REMR, SML_SFLCT and the proposed image fusion algorithms
 respectively; Difference images between clockB image and the listed fused images.

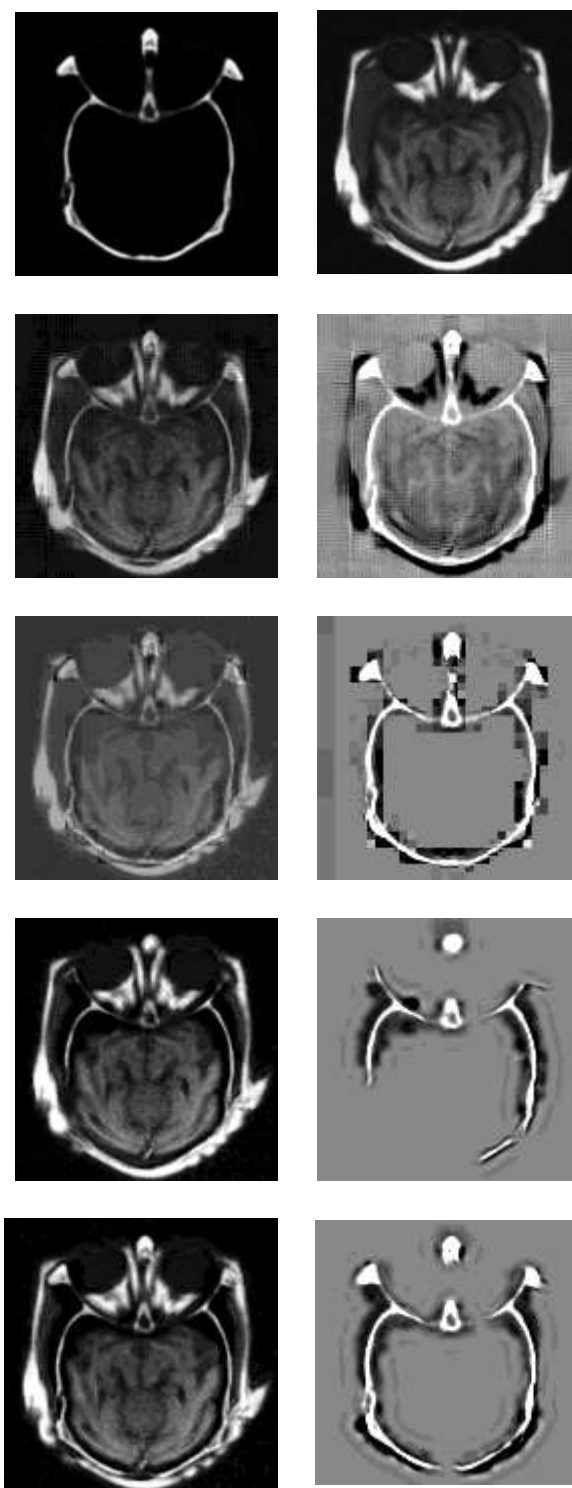


Figure 6. Medical image fusion results

From top left corner to bottom right corner:CT image; MRI image; Fused medical images using GEB, REMR, SML_ SFLCT and the proposed image fusion algorithms respectively; Difference images between CT image and the listed fused images.

We also apply the proposed method in medical image fusion. A CT image that shows structures of bone, while MRI image shows areas of soft tissue. However, in clinical applications, doctors need to see the position of both bone and tissue to determine pathology and aid in diagnosis. So the mixed image is usually needed in practice, which includes as much of the information in CT and MRI as possible. The fusion results are shown in figure.6. From figure.6, it is clear that fused image of GEM fusion method is quite blurry and contains artificial textures; The fused image of REMR method yields blocks aliasing phenomenon. and the fused image constructed by SML_SFLCT method is inaccurate for losing some details of source CT image. Obviously, our proposed method is superior to others.

VI. CONCLUSIONS

In this paper we first proposed a novel scheme with joint NSCT and OCBT. This proposed MSD transform not only can represent the geometrical features such as edges and textures more sparsely but also capture and preserve the anisotropic edge information and detail direction textures of collected images effectively. In terms of these excellent properties, we apply it in fusing multifocus and medical images, and employ the hybrid region and pixel energy features as the fused strategy.

In this way, we overcome the disadvantages of traditional region-based fusion methods in MSD domain and achieved a good image fusion performance. The simulation results indicated that the proposed method is visually superior to others in preserving details and textures in the fused images and also achieved the largest MI and $Q^{AB/F}$ values.

REFERENCES

- [1] Qu Xiao-Bo, Yan Jing-Wen, Zhu Zi-Qian, Chen Ben-Gang. "Multipulse coupled neural networks". In Proceedings of International Conference on Bio-Inspired Computing Theories and Applications. Zhengzhou, China: Publishing House of Electronics Industry. 2007, pp.563-565.
- [2] M N Do, M Vetterli. "The contourlet transform: an efficient directional multiresolution image representation" [J]. IEEE Transactions on Image Processing, Vol 14, No. 10. 2005, pp.2091-2106.

- [3] Arthur L. da Cunha, Jianping Zhou.” The Nonsampled Contourlet Transform: Theory, Design, and Applications”. IEEE Transactions on Image Processing, Vol 15, No. 10, October, 2006.
- [4] F. G. Meyer and R. R. Coifman. “Brushlet: A tool for directional image analysis and image compression”. Applied and Computational Harmonic Analysis, Vol 4, 1997, pp.147–187.
- [5] Mingxin Yang, “Optimal Cluster Head Number Based On Enter For Datd Aggregation In Wireless Sensor Networks”, International Journal on Smart Sensing and Intelligent Systems (S2IS), Dec 2015, pp.1935 – 1955
- [6] Ahadul Imam, Justin Chi, Mohammad Mozumdar, ”Data Compression And Visualization For Wireless Sensor Networks ” International Journal on Smart Sensing and Intelligent Systems (S2IS), Dec 2015, pp.2083- 2115
- [7] Payman Moallem1, ”Compensation Of Capacitive Differential Pressure Sensor Using Multi Layer Perceptron Neural Network”, International Journal on Smart Sensing and Intelligent Systems (S2IS), SEPTEMBER 2015, pp.1443 – 1463
- [8] Daode Zhang, Yangliu Xue, Xuhui Ye and Yanli Li. ”Research On Chips’ Defect Extraction Based On Image-matching ”, International Journal on Smart Sensing and Intelligent Systems (S2IS), Mar. 10. 2014, pp.321 – 336
- [9] Feng LUO and Fengjian HU, ”A Comprehensive Survey Of Vision Based Vehicle Intelligent Front Light System ” International Journal on Smart Sensing and Intelligent Systems (S2IS), June 1. 2014, pp.701 – 723
- [10] E. Angelini, A. Laine, et. al. ”LV volume quantification via spatio temporal analysis of real-time 3D echocardiography”. IEEE Transactions on Medical Imaging. Vol. 20, No.6, 2001, pp.457-469.
- [11] Guohui Wu, Xingkun Li, Jiyang Dai. ”Improved Measure Algorithm Based On CoSaMP For Image Recovery ” International Journal on Smart Sensing and Intelligent Systems (S2IS), June 1. 2014, pp.724 – 739
- [12] Wenqing Chen, 2 Tao Wang and 3 Bailing Wang. ”Design Of Digital Image Encryption Algorithm Based On Mixed Chaotic Sequences”. International Journal on Smart Sensing and Intelligent Systems (S2IS), Dec. 1. 2014, pp.1453 – 1469
- [13] S.Mary Praveena, Dr. I.L.A. Vennila. ” Image Fusion By Global Energy Merging”. International Journal of Recent Trends in Engineering, Vol 2, No. 7, November 2009.

- [14] Zhouping Y. “Fusion Algorithm Of Optical Images And Sar With Svt And Sparse Representation”. International Journal on Smart Sensing and Intelligent Systems, Vol. 8, No. 2, June 2015.
- [15] Yongqing Wang, “New Intelligent Classification Method Based On Improved Meb Algorithm”, International Journal on Smart Sensing and Intelligent Systems, Vol. 7, No. 1, 2014, pp. 72-95.
- [16] Yongqing Wang¹ and Xiling Liu.”Face Recognition Based On Improved Support Vector Clustering ”International Journal on Smart Sensing and Intelligent Systems (S2IS), Dec. 1. 2014,pp.1807 – 1829
- [17] Donoho D L, “Compressed sensing”, IEEE Transactions on Information Theory, vol. 52, No. 4, 2006, pp. 1289-1306.
- [18] Yang C, Wright J, Huang T, Ma Y “Image super-resolution via sparse representation”.IEEE Trans. Image Process, vol. 19, No. 11, 2010, pp. 2861-2873.
- [19] James E. Fowler, Sungkwang Mun, and Eric W. Tramel,Multi-scale block compressed sensing with smoothed projected landweber reconstruction, 19th European Signal Processing Conference, Barcelona, Spain,2011.
- [20] Easley G, Labate D, Lim W.”Sparse Directional image representations using the discrete Shearlet transform”.Applied and Computational Harmonic Analysis, Vol. 7, 2008,pp.25-46.
- [21] Do T T, Tran T D, Lu G. “Fast compressive sampling with structurally random matrices”, Proceedings of the IEEE International Conference on Acoustics, Speech and Signal Processing. Washington D C: IEEE Computer Society Press, 2008,pp.3369-3372.
- [22] Chen SSB, Donoho D L, M A Saunders. “Atomic decomposition by basis pursuit”, SIAM Journal on Scientific Computation, vol. 20, No. 1, 2010, pp. 33-61.
- [23] Tropp J A. “Greed is good: Algorithmic results for sparse approximation”. IEEE Transactions on Information Theory, vol. 50, No. 10, 2004, pp. 2231-2242.
- [24] Blumensath T, Davies M E,Normalised , “iterative hard thresholding:guaranteed stability and performance”,IEEE Journal of Selected Topics in Signal Processing, vol. 4, No. 2, 2010, pp. 298–309.
- [25] Bai Q, Jin C. “Image Fusion And Recognition Based On Compressed Sensing Theory”. International Journal on Smart Sensing & Intelligent Systems, Vol. 8, No. 1, 2015.

[26] Petrovic V, Xydeas C. "On the effects of sensor noise in pixel-level image fusion performance". In: Proceedings of the 3rd International Conference on Image Fusion. Paris, France:IEEE, 2000,pp.14-19.